• At perihelion and aphelion, the velocities are purely tangential (circular) so that their values lead to the determination of L in terms of a and e:

$$L \;=\; \mu r_p v_p \;=\; \mu r_a v_a \quad \Rightarrow \quad \frac{v_p}{v_a} \;=\; \frac{r_a}{r_p} \;=\; \frac{1+e}{1-e} \quad . \tag{45}$$

Insertion into the energy equation

$$\frac{1}{2}\mu v_p^2 - G\frac{M\mu}{a(1-e)} \;=\; \frac{1}{2}\mu v_a^2 - G\frac{M\mu}{a(1+e)} \tag{46}$$

which rearranges to

$$\frac{1}{2}\mu v_p^2 \left\{ 1 - \left(\frac{1-e}{1+e} \right)^2 \right\} \;=\; \frac{GM\mu}{a} \left(\frac{1}{1-e} - \frac{1}{1+e} \right) \quad . \tag{47}$$

Eliminating v_p then yields the result

$$L \;=\; \mu\sqrt{GMa(1-e^2)} \quad , \tag{48}$$

so that for fixed a, the angular momentum is maximized for circular orbits. While this demonstrates the facility of considering orbits at perihelion and aphelion, this result could be simply obtained directly from Eq. (40).

6.3 Kepler's Third Law

This law follows immediately from his second law, i.e. by integrating Eq. (44) over an entire period P, for which the time integration is trivial. Since the area of the ellipse is $\pi ab = \pi a^2\sqrt{1-e^2}$, this can be equated to $LP/(2\mu)$ using Eq. (48) to yield

$$\boxed{\frac{a^3}{P^2} \;=\; \frac{GM}{4\pi^2}} \tag{49}$$

as the general form of **Kepler's Third Law** for $e \neq 0$. Here $M = m_1 + m_2$, so that the total mass of the system determines the period.

$*$ This law is used ubiquitously in astrophysics as a means of mass determination; for example black holes.

2. BINARY STARS, EXOPLANETS AND THE VIRIAL THEOREM

Matthew Baring – Lecture Notes for ASTR 350, Fall 2021

1 Binary Stars

Binary stellar systems are another showcase for the application of Kepler's laws. We identify 4 main classes of binaries:

C & O, Chap. 7

• *Visual binaries* — we can see both members moving in ellipses; resolved at most or all times.

• *Astrometric binaries* — we can see one very bright member and can infer the presence of the other companion (faint star) from the bright one's elliptical orbit.

• *Eclipsing binaries* — one companion passes in front of and behind the other: orbital plane is approximately along the line of sight.

• *Spectroscopic binaries* — spectra of two discernible binary stars periodically redshift and blueshift according to orbital phase.

∗ These last two cases constitute the principal tools astronomers use for searching for extrasolar planets.

Plot: Astrometric and eclipsing binaries

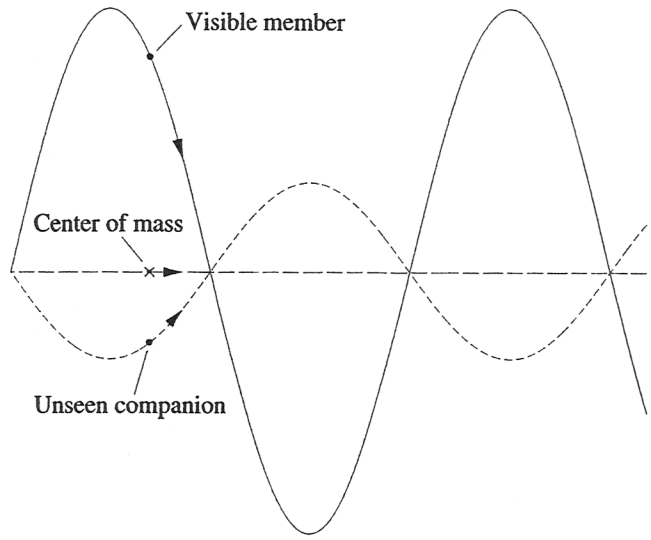

Figure 7.1 An astrometric binary, which contains one visible member. The unseen component is implied by the oscillatory motion of the observed element of the system.

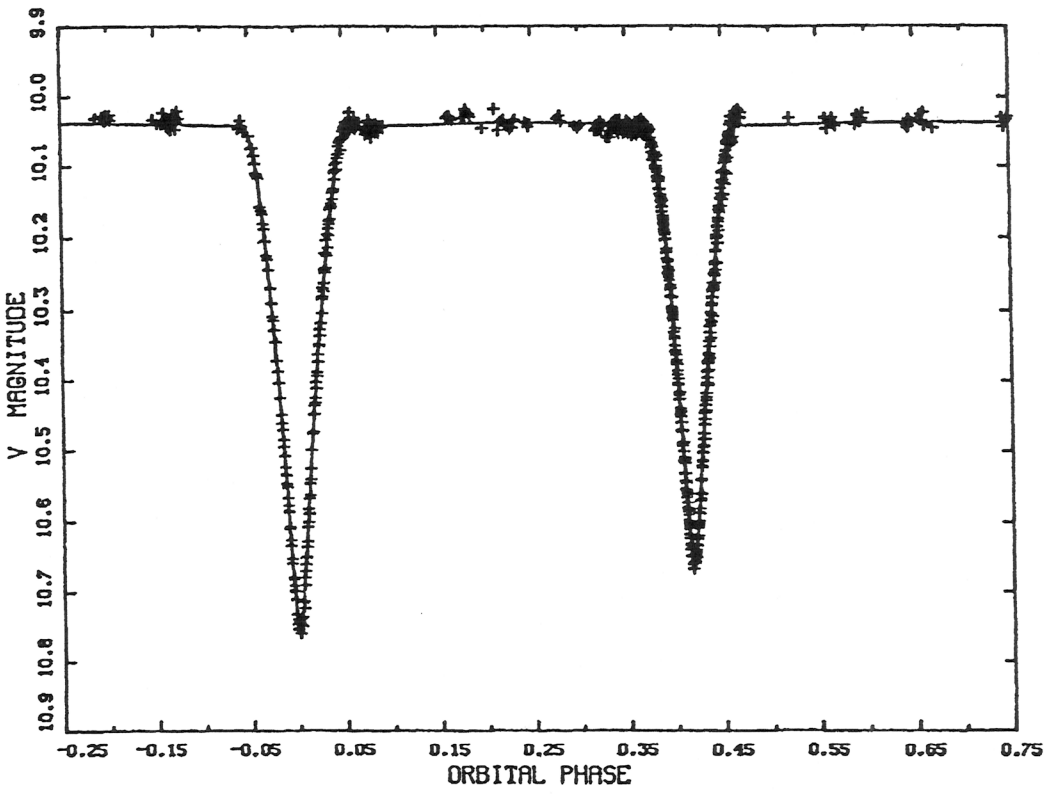

Figure 7.2 The V magnitude light curve of YY Sagittarii, an eclipsing binary star. The data from many orbital periods have been plotted on this light curve as a function of phase, where the phase is defined to be 0.0 at the primary minimum. This system has an orbital period $P = 2.6284734$ d, an eccentricity $e = 0.1573$, and orbital inclination $i = 88.89°$ (see Section 7.2). (Figure from Lacy, C. H. S., *Astron. J.*, *105*, 637, 1993.)

1.1 Mass Determination Using Visual Binaries

C & O, Sec. 7.2

The goal here is to discern how knowledge of elliptical orbits for both members can constrain their masses. In CM coordinates, $m_1\vec{r}_1 + m_2\vec{r}_2 = \vec{0}$. The ellipses then establish

$$m_1 a_1 \;=\; m_2 a_2 \quad . \tag{1}$$

If d is the (unknown) distance to the binary, then the angles subtended by a_1 and a_2 are

$$\alpha_1 \;=\; \frac{a_1}{d} \quad , \quad \alpha_2 \;=\; \frac{a_2}{d} \quad , \tag{2}$$

which leads to the determination of the mass ratio:

$$\frac{m_2}{m_1} \;=\; \frac{\alpha_1}{\alpha_2} \quad . \tag{3}$$

- If the plane of the orbit is tipped by an inclination angle i from *the plane of the sky*, then the projected angles are $\tilde{\alpha}_i$ (measured quantities), so that

$$\frac{m_2}{m_1} \;=\; \frac{\alpha_1}{\alpha_2} \;=\; \frac{\tilde{\alpha}_1/\cos i}{\tilde{\alpha}_2/\cos i} \;=\; \frac{\tilde{\alpha}_1}{\tilde{\alpha}_2} \quad , \tag{4}$$

i.e., orbital inclination effects cancel and do not affect the **mass ratio** determination.

- This cancellation does not occur when applying Kepler's Third Law:

$$P^2 \;=\; \frac{4\pi^2 a^3}{G(m_1 + m_2)} \quad , \quad a \;=\; a_1 + a_2 \quad . \tag{5}$$

Each star has the same period P in its orbit, so if this is measured and the distance d to the source is known, then we know a_1, a_2 and a (for $\cos i = 1$), and hence $m_1 + m_2$, i.e., the **total mass**.

- Information on $m_1 + m_2$ and m_1/m_2 yields each mass separately.

- In general, we do not know $\cos i$, though eclipsing constrains it to values much less than unity, for which *orbital parameters are not as well determined.*

• For $\tilde{\alpha} = \tilde{\alpha}_1 + \tilde{\alpha}_2$, Kepler III gives

$$m_1 + m_2 \;=\; \frac{4\pi^2}{G}\,\frac{(\alpha d)^3}{P^2} \;=\; \frac{4\pi^2}{G}\left(\frac{d}{\cos i}\right)^3 \frac{\tilde{\alpha}^3}{P^2} \quad . \tag{6}$$

Information on $\cos i$ can be obtained by probing the offset of the focus of the projected ellipse from dynamical determinations for the true ellipse.

∗ Tipping of the ellipse around the semi-major axis can confuse the picture.

Plot: Binary orbit projections

1.2 Spectroscopic and Eclipsing Binaries

• Adding information concerning spectral lines or from eclipses can constrain the system further, deducing individual masses, and perhaps even radii and effective temperatures. **C & O, Sec. 7.3**

• Doppler effect probes radial (line of sight; LOS) velocity, i.e., $v_{1r} = v_1 \sin i$ and $v_{2r} = v_2 \sin i$.

∗ This works best for orbital planes perpendicular to the sky, i.e. along the LOS.

• For circular orbits, regardless of the value of $\cos i$, the spectroscopic velocity curves are *sinusoidal* in time (since $d\theta/dt =$ const.), with the amplitude for both stars modulated by $\sin i$.

• Eccentric orbits ($e \neq 0$) will skew and distort the velocity time profiles: sinusoidal signatures in θ map over to distinctive curves in t due to the transcendental relationship between θ and t .

∗ the distortion depends on $\sin i$ and the orientation of the semi-major axis $\Rightarrow$ a wealth of information can be gleaned from the light curves.

Plot: Radial velocity curves

Binary Orbit Projections

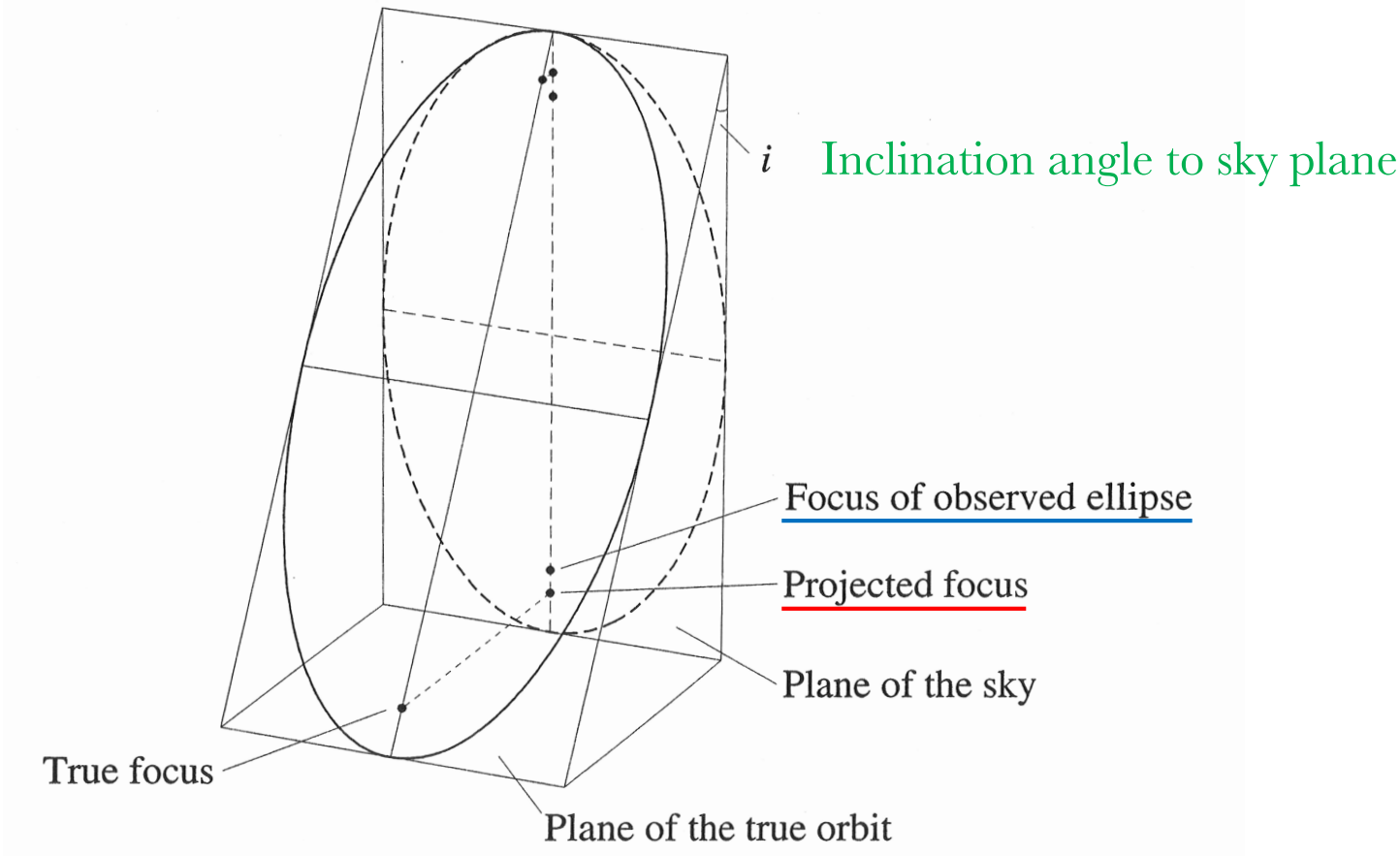

- An elliptical orbit projected onto the plane of the sky is an ellipse. The foci of the projected true ellipse are offset along the major axis from the foci of the observed ellipse.
- The inclination angle i can be determined using precise orbital timing. A prime application is star S2 around the supermassive black hole Sgr A* at the Galactic centre.

Spectroscopic Binaries

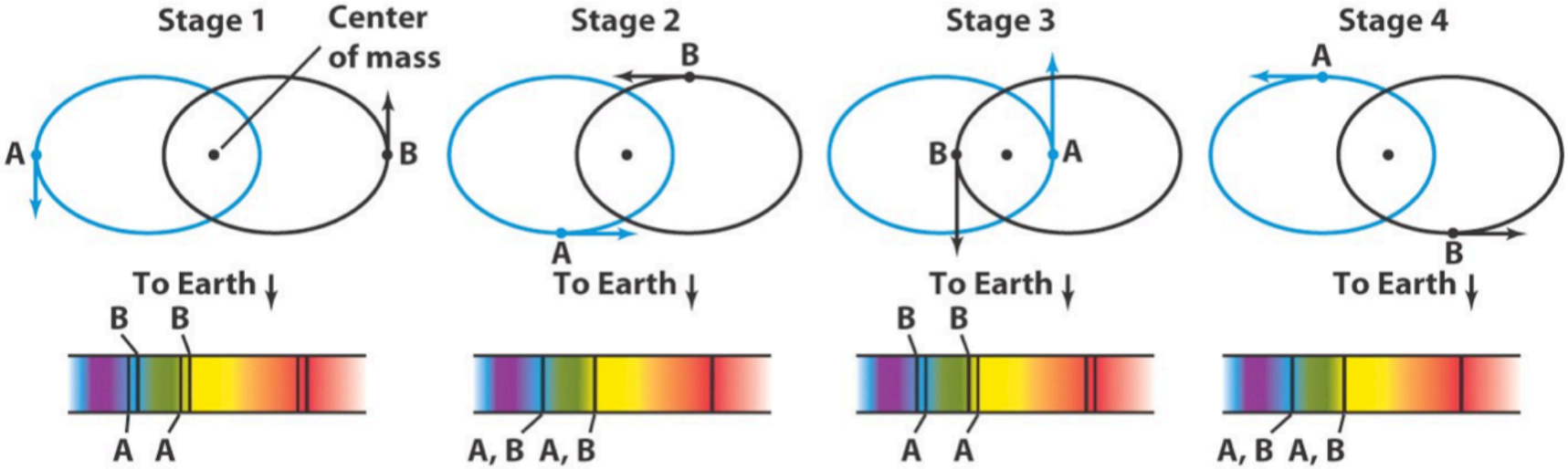

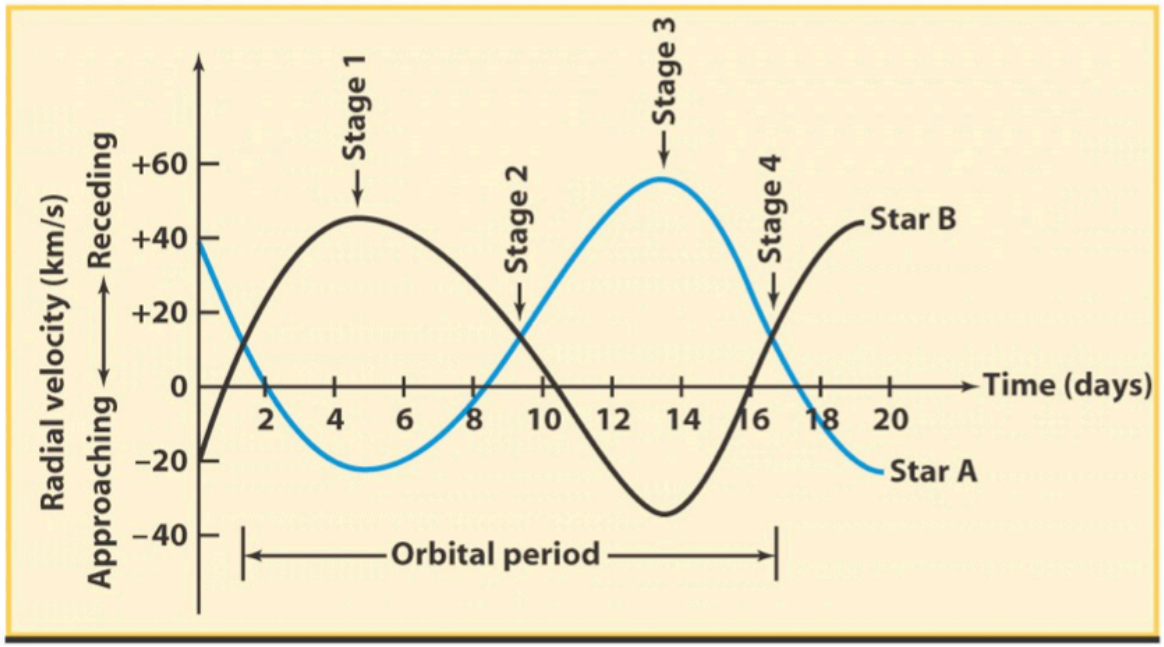

Velocity curves for a spectroscopic binary

Graphics courtesy of Caltech Astronomy

• In practice, tidal interactions tend to circularize the orbits, so that often $e \approx 0$. Then

$$v_1 \;=\; \frac{2\pi a_1}{P} \quad , \quad v_2 \;=\; \frac{2\pi a_2}{P} \tag{7}$$

and

$$\frac{m_1}{m_2} \;=\; \frac{a_2}{a_1} \;=\; \frac{v_2}{v_1} \;=\; \frac{v_{2r}/\sin i}{v_{1r}/\sin i} \;=\; \frac{v_{2r}}{v_{1r}} \tag{8}$$

where subscripts r denote radial velocities. Hence, *the mass ratio is determined by Doppler spectroscopic observables.* Working with Kepler III then gives

$$a \;=\; a_1 + a_2 \;=\; \frac{P}{2\pi}\,(v_1 + v_2) \tag{9}$$

so that

$$\begin{aligned} m_1 + m_2 \;&=\; \frac{4\pi^2 a^3}{GP^2} \;\equiv\; \frac{P}{2\pi G}\,(v_1 + v_2)^3 \\ &=\; \frac{P}{2\pi G}\,\frac{(v_{1r} + v_{2r})^3}{\sin^3 i} \;=\; \frac{P}{2\pi G}\,\frac{v_{1r}^3}{\sin^3 i}\left(1 + \frac{m_1}{m_2}\right)^3 \quad . \end{aligned} \tag{10}$$

Hence,

$$\boxed{\frac{m_2^3}{(m_1 + m_2)^2}\;\sin^3 i \;=\; \frac{P}{2\pi G}\,v_{1r}^3 \quad .} \tag{11}$$

The L.H.S. of this equation is know as the **mass function**, and the R.H.S. comprises observables, even in cases where one companion is too faint to be observed (so-called *single-line spectroscopic binaries*).

• Often, the mass function is used to establish a lower bound on m_2 (using $\sin i = 1$), if the mass ratio cannot be determined.

∗ This approach is particularly useful for identifying candidate black holes.

Plot: Table of Galactic Black Hole Candidates

• Dynamical estimates of single-line spectroscopic binaries can rule out neutron stars or white dwarfs as companions because of high inferred masses.

Black Hole Masses in Binaries

Table 4.2. *Confirmed black hole binaries: X–ray and optical data*

Source	f(M)[a] ($M_\odot$)	M_1^a ($M_\odot$)	f(HFQPO) (Hz)	f(LFQPO) (Hz)	Radio[b]	E^c_{max} (MeV)	References
0422+32	1.19±0.02	3.2–13.2	–	0.035–32	P	0.8,1–2:	1,2,3,4,5
0538–641	2.3±0.3	5.9–9.2	–	0.46	–	0.05	6,7
0540–697	0.14±0.05	4.0–10.0:	–	0.075	–	0.02	8,7
0620–003	2.72±0.06	3.3–12.9	–	–	P,J?	0.03:	9,10,11,11a
1009–45	3.17±0.12	6.3–8.0	–	0.04–0.3	–[d]	0.40, 1:	12,4,13
1118+480	6.1±0.3	6.5–7.2	–	0.07–0.15	P	0.15	14,15,16,17
1124–684	3.01±0.15	6.5–8.2	–	3.0-8.4	P	0.50	18,19,20,21
1543–475	0.25±0.01	7.4–11.4[e]	–	7	–[f]	0.20	22,4
1550–564	6.86±0.71	8.4–10.8	92,184,276	0.1-10	P,J	0.20	23,24,25,26,27
1655–40	2.73±0.09	6.0–6.6	300,450	0.1–28	P,J	0.80	28,29,30,31,54
1659–487	$> 2.0^g$	–	–	0.09–7.4	P	0.45, 1:	32,33,4,13
1705–250	4.86±0.13	5.6–8.3	–	–	–[d]	0.1	34,35
1819.3–2525	3.13±0.13	6.8–7.4	–	–	P,J	0.02	36,37
1859+226	7.4±1.1	7.6–12:	190	0.5–10	P,J?	0.2	38,39,40,41
1915+105	9.5±3.0	10.0–18.0:	41,67,113,168	0.001-10	P,J	0.5, 1:	42,43,44,4,13
1956+350	0.244±0.005	6.9–13.2	–	0.035–12	P,J	2–5	45,46,47,48,49
2000+251	5.01±0.12	7.1–7.8	–	2.4–2.6	P	0.3	18,50,51
2023+338	6.08±0.06	10.1–13.4	–	–	P	0.4	52,53

- Dynamical estimates of Galactic black hole masses (highlighted M_1 column) – cases confirmed by radio and optical observations of the orbiting companion.
- From McClintock and Remillard (2004) in "Compact Stellar X-ray Sources," eds. W.H.G. Lewin & M. van der Klis, Cambridge University Press. [astro-ph/0306213]

• Information on $\sin i$ is available in eclipsing systems:

∗ deep eclipses have flat bottoms, implying $\sin i \approx 1$;

∗ particle eclipses have no flat bottoms and smoother onsets, implying $0.8 \lesssim \sin i \lesssim 0.9$.

Plot: Eclipse time profiles

• The duration of eclipses, coupled with dynamical information on v_i, lead to determinations of the **radius** of the obscured companion, and also the obscuring companion:

$$\begin{aligned} r_s &= \frac{v}{2}(t_b - t_a) \\ r_l &= \frac{v}{2}(t_c - t_a) \;=\; r_s + \frac{v}{2}(t_c - t_b) \end{aligned} \tag{12}$$

for the radii r_s and r_l for the smaller and larger binary member, respectively.

∗ Given flux measurements and spectroscopic T, this can be used to determine stellar distances via the Stefan-Boltzmann law.

[*Reading Assignment: C & O: pp. 192–193 on temperature properties and distance inferences from brightness measurements*]

Eclipsing Binaries

Light curve depends on orbital inclination and phase

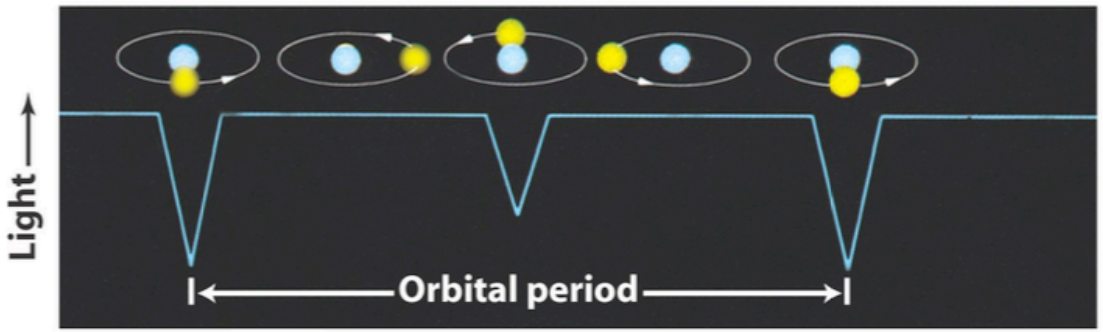

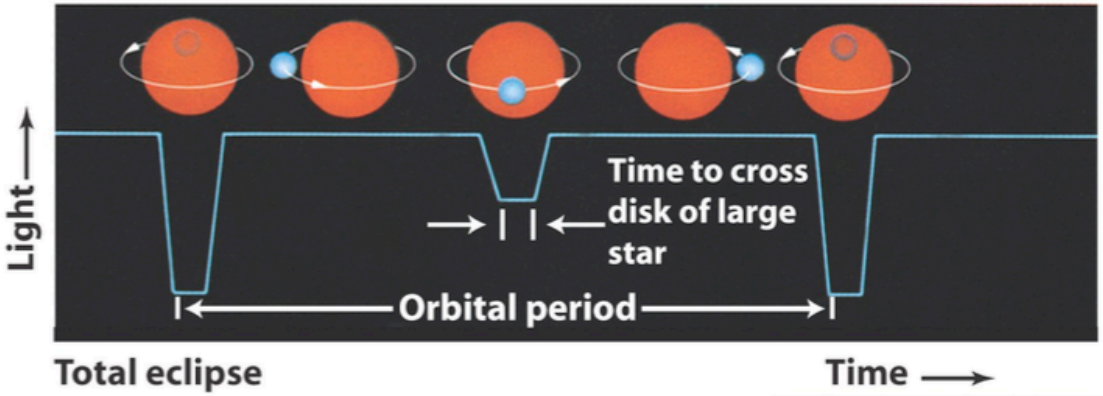

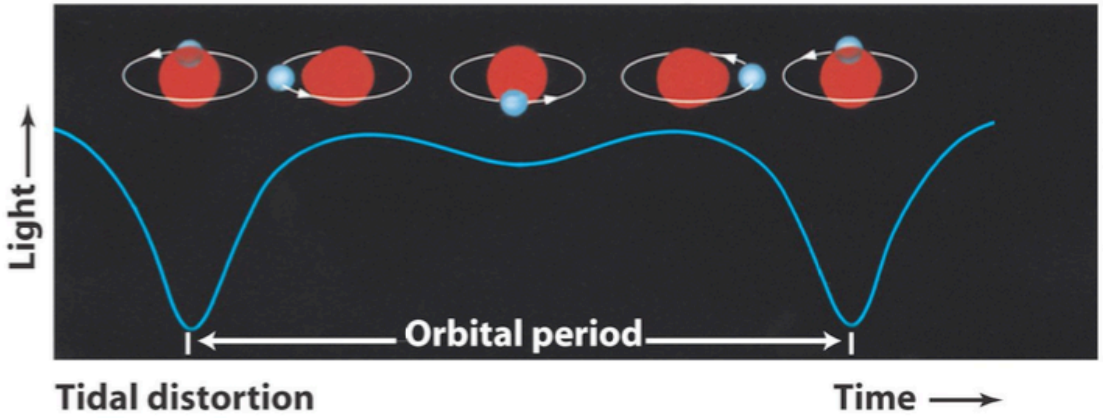

Graphics courtesy of NASA GSFC and Caltech Astronomy